

Another structural comparison is with the recent structure¹³ of bis(ethylene)(tricyclohexylphosphine)nickel. The pertinent data for that structure are 1.401 (14) Å for C=C, 2.014 (11) Å for Ni-C, and 2.196 (2) Å for Ni-P. These data are very similar to the data for (C₂H₄)Ni[(C₆H₅)₃P]₂ and minor differences can be attributed to the fact that this structure has one phosphine and two olefin ligands. The longer Ni-P distance in the tricyclohexylphosphine structure (2.196 (2) vs. 2.152 (5) Å) is consistent with the reasonable possibility for reduced π -acceptor properties of the phosphine ligand.

All Ni(0)- and Pt(0)-olefin complexes (Table XII) have the olefin ligand approximately in the PNiP plane (dihedral angle near 0°), whereas all comparable Pt(II) complexes have the olefin approximately perpendicular to this plane (dihedral angle near 90°). Mason³⁶ has suggested that the reason for this is that lowering the energy of the Pt p_z orbital

in the 2+ oxidation state increases its involvement in bonding favoring a dihedral angle of 90°. Wheelock,³⁷ *et al.*, have been able to reproduce the position of the observed energy minimum with semiempirical molecular orbital calculations. The implication from their work seems to be that the small difference in energy between the two conformations is a net effect, difficult to pin down simply. In any case the 0 or 90° dihedral angle can hardly be a steric effect and the underlying reasons for the preferred conformation are still obscure.

Registry No. (C₂H₃CN)Ni[o-CH₃C₆H₄O]₃P]₂, 31666-48-5; (C₂H₄)Ni[o-CH₃C₆H₄O]₃P]₂, 31666-47-4.

Acknowledgment. I wish to thank C. A. Tolman and W. C. Seidel for crystals and L. F. Lardear for help with the film work and figures.

(37) K. S. Wheelock, J. A. Nelson, L. C. Cusachs, and H. B. Jonassen, *J. Amer. Chem. Soc.*, **92**, 5110 (1970).

(36) R. Mason and G. B. Robertson, *J. Chem. Soc. A*, 492 (1969).

Contribution No. 1950 from the Central Research Department, Experimental Station, E. I. du Pont de Nemours and Company, Wilmington, Delaware 19898

Crystal Structure and Single-Crystal Electron Paramagnetic Resonance Data for Bis[dihydrobis(1-pyrazolyl)borato]cobalt(II)

L. J. GUGGENBERGER,* C. T. PREWITT, P. MEAKIN, S. TROFIMENKO, and J. P. JESSON*

Received August 2, 1972

The molecular and crystal structures of bis[dihydrobis(1-pyrazolyl)borato]cobalt(II), [H₂B(pz)₂]₂Co, have been determined from X-ray diffractometer data. Crystals are orthorhombic, in the polar space group *Pc2₁b* (nonstandard setting of *Pca2₁*), with cell dimensions of *a* = 11.200 (12), *b* = 14.268 (15), and *c* = 10.216 (12) Å. The observed and calculated densities for four molecules per cell are 1.44 and 1.43 g/cm³, respectively. The structure was solved by Patterson superposition and Fourier techniques and refined by least squares to a conventional *R* of 0.065. The crystal structure consists of the packing of discrete molecules which have two bidentate dihydro(1-pyrazolyl)borato ligands, [H₂B(pz)₂]⁻, bonded to cobalt. The local cobalt atom coordination is a distorted tetrahedron with Co-N distances of 1.967 (12) Å, whereas the overall molecular symmetry is only approximately C₂(2). Paramagnetic resonance data obtained on magnetically dilute systems at 4.2°K are presented for the parent complex and some substituted derivatives. In contrast to the corresponding bis[hydrotris(1-pyrazolyl)borato]cobalt(II) complexes, there are sizable changes in the apparent *g* values and hyperfine coupling constants with substitution. The resonance spectra are notable for the fact that it appears that only the ±³/₂ transition of the ⁴A₂ ground state is observed and, for this reason, they can only be partially analyzed.

Introduction

Numerous transition metal polypyrazolylborates of the types M[R₂B(pz)₂]₂ and M[RB(pz)₃]₂ have been synthesized.^{1,2} The pyrazolylborato ligands R₂B(pz)₂⁻ and RB(pz)₃⁻ usually act as bidentate or tridentate chelating ligands, respectively, on coordination with transition metals. A variety of complexes are formed with the divalent transition metal ions having different metal atom configurations and coordination geometries yet maintaining fairly constant ligand characteristics. Optical, nmr, epr, Mossbauer, and magnetic susceptibility data have been reported for some of them.³⁻⁹

We report here the molecular and crystal structures of bis[dihydrobis(1-pyrazolyl)borato]cobalt(II), [H₂B(pz)₂]₂Co. This structure serves as a model for the tetrahedral transition metal-bis(1-pyrazolyl)borato complexes (Mn²⁺, Fe²⁺, Co²⁺, Zn²⁺). The remaining bis(1-pyrazolyl)borato complexes have an essentially square-planar metal atom configuration.⁴

Comparisons are made with the structural data from the bidentate H₂B[3,5-(CH₃)₂pz]₂Mo(CO)₂- π -C₃H₅¹⁰ and H₂B[3,5-(CH₃)₂pz]₂Mo(CO)₂(C₇H₇)¹¹ structures and the tridentate [HB(pz)₃]₂Co,¹² HB(pz)₃Mo(CO)₂N₂C₆H₅,¹³ and HB(pz)₃(COCH₃)Fe(CO)₂¹⁴ structures.

(8) J. P. Jesson, J. F. Weiher, and S. Trofimenko, *J. Chem. Phys.*, **48**, 2058 (1968).

(9) G. N. La Mar, J. P. Jesson, and P. Meakin, *J. Amer. Chem. Soc.*, **93**, 1286 (1971).

(10) C. A. Kosky, P. Ganis, and G. Avitabile, *Acta Crystallogr. Sect. B*, **27**, 1859 (1971).

(11) F. A. Cotton, M. Jeremic, and A. Shaver, *Inorg. Chim. Acta*, in press.

(12) M. R. Churchill, K. Gold, and C. E. Maw, Jr., *Inorg. Chem.*, **9**, 1597 (1970).

(13) G. Avitabile, P. Ganis, and M. Nemiroff, *Acta Crystallogr. Sect. B*, **27**, 725 (1971).

(1) S. Trofimenko, *J. Amer. Chem. Soc.*, **88**, 1842 (1966).

(2) S. Trofimenko, *J. Amer. Chem. Soc.*, **89**, 3170, 6288 (1967).

(3) J. P. Jesson, *J. Chem. Phys.*, **45**, 1049 (1966).

(4) J. P. Jesson, S. Trofimenko, and D. R. Eaton, *J. Amer. Chem. Soc.*, **89**, 3148, (1967).

(5) J. P. Jesson, S. Trofimenko, and D. R. Eaton, *J. Amer. Chem. Soc.*, **89**, 3158 (1967).

(6) J. P. Jesson, *J. Chem. Phys.*, **47**, 582 (1967).

(7) J. P. Jesson and J. F. Weiher, *J. Chem. Phys.*, **46**, 1995 (1967).

The initial impetus for the X-ray study was to define the molecular geometry so that, in combination with epr and nmr measurements, the dipolar and contact contributions to the nuclear resonance shifts of the protons in the ligand could be separated. This separation had previously been definitively achieved for the corresponding tris-pyrazolyl complexes.^{3,6,9,15} Complications occur in the tetrahedral systems which have so far prevented a separation of the two effects. The crystal structure information and problems associated with the epr approach to defining the magnetic properties of the central ion are discussed below.

Experimental Section

A. Crystal Data and Structure Determination. Crystals of $[H_2B(pz)_2]_2Co$ are orthorhombic with cell parameters of $a = 11.200$ (12), $b = 14.268$ (15), and $c = 10.216$ (12) Å. These parameters are averages of film and diffractometer measured values. The observed and calculated densities for four molecules per cell are 1.44 and 1.43 g/cm³, respectively. The systematic absences of $hk0$, $k = 2n + 1$, and $0kl$, $l = 2n + 1$, uniquely establish the space group as $Pc2_1b$ (nonstandard setting for $Pca2_1$).¹⁶ All atoms are in the general positions $(x, y, z; \bar{x}, 1/2 + y, \bar{z}; \bar{x}, y, 1/2 + z; x, 1/2 + y, 1/2 - z)$. The nonstandard setting was maintained to remain consistent with parallel work being done on single-crystal epr.

The crystal chosen for data collection was needlelike with dimensions of $0.2 \times 0.4 \times 0.7$ mm with a somewhat irregular cross section. The data were collected on a Picker four-circle diffractometer with the 001 needle axis coincident with the diffractometer ϕ axis. The θ - 2θ scan technique was used with Zr-filtered Mo radiation (λ 0.7107 Å). The scan range was 3° plus the angular separation of $K\alpha_1$ and $K\alpha_2$ with individual backgrounds of 20 sec measured before and after each scan. A total of 1250 reflections were measured; this included standard reflections and some duplicate reflections which were averaged.

The data were corrected for Lorentz and polarization effects in the usual way. The structure factors which were less than their estimated standard deviations were called "unobserved."¹⁷ Several types of absorption corrections were made. Although the linear absorption coefficient for Mo $K\alpha$ radiation is only 11 cm⁻¹, it is a significant effect here because of the large crystal used. The initial absorption correction was done using the program ACACA¹⁸ with the crystal defined by six plane faces. Several crystal shape parameters were tried but we were unable adequately to reproduce the ϕ dependence of the transmission. The final refinements were done after applying an empirical absorption correction based on the experimentally observed ϕ dependence of the transmission. This was done by rotating about the 004 reciprocal lattice vector at $\psi = 90^\circ$; in this geometry the variation in integrated intensities is due, in a first-order approximation, to absorption effects. The observed variation in the transmission factor in the ϕ range used was a smooth function with a minimum transmission at one end of the range, a maximum in the middle, and an intermediate value at the other end of the range. The maximum observed deviation in the transmission was 24%.

A sharpened Patterson function was calculated from which the cobalt atom position was determined. The superposition function in conjunction with the minimum function was used to find the nitrogen atom positions. These atoms were used to phase an electron density difference map on which all the remaining nonhydrogen atoms were located. The R factor $(\sum |F_o| - |F_c|) / \sum |F_o|$ after several cycles of isotropic refinement was 0.091. The best agreement we obtained using these data (corrected using calculated transmission factors) was an R of 0.081 after full anisotropic refinement. The variables in all the anisotropic refinements were varied in two non-overlapping groups. The first group contained the positional and thermal parameters for the cobalt atom, eight nitrogen atoms, and two boron atoms; the second group contained all the parameters for the twelve carbon atoms.

A new refinement was initiated with the data corrected empirically for absorption (*vide supra*). The new isotropic refinement gave an R of 0.08; the new anisotropic refinement gave an R of 0.079 and a R_w $\{[\sum w(|F_o| - |F_c|)^2] / \sum w |F_o|^2\}^{1/2}$ of 0.052. The hydrogen atoms were placed in their calculated positions after observing evidence for them in an electron density difference map. The hydrogen atom thermal parameters were set at 4.0 Å²; none of the hydrogen atom positional or thermal parameters were varied. The final agreement after several additional cycles of refinement was 0.065 for R and 0.041 for R_w for 1132 observed reflections. The values for R and R_w for all the data (1201 reflections) are 0.083 and 0.066, respectively. The "error of fit" was 0.94 for both refinement groups.

The space group $Pc2_1b$ is polar in the b direction so that there is a question with regard to which way the molecule is pointing relative to the polar axis. Several refinement cycles were done with the molecule pointing in the opposite direction with final values for the observed data of 0.069 for R and 0.044 for R_w and 1.01 for the "error of fit." The agreement for the previous orientation is significantly¹⁹ better than for this orientation, and we conclude that the original orientation was correct with respect to the polar axis.

We feel the refinement with the "φ-only" empirical absorption correction is slightly better than the best refinement using calculated transmission factors. Henceforth, all the parameters reported are those resulting from the final refinements with the empirically corrected data. The agreement between chemically equivalent distances was about the same in both refinements and, in general, the overall differences between the refinements are minor. There were some differences in individual distances, but the average distances are essentially unaffected. We concluded that the structure refinement is limited by the absorption correction and this is the main cause for the rather large deviations observed for some chemically equivalent distances and angles.

Atomic scattering factors for the neutral atoms were used.²⁰ The cobalt atom was corrected for the real and imaginary parts of the anomalous scattering effect.²¹ The least squares minimized the function $\sum w(|F_o| - |F_c|)^2$.

The final refined positional parameters are given in Table I and the thermal parameters in Table II. A list of observed and calculated structure factors is available.²²

B. Paramagnetic Resonance Data. Single-crystal and powder studies have been carried out on magnetically dilute samples of $[H_2B(pz)_2]_2Co$, as well as studies on magnetically dilute powders of a number of substituted derivatives of the parent complex. In all cases the corresponding zinc complex was used as the host lattice. Crystals were grown by slow evaporation from chloroform solution. Single-crystal X-ray photographs were taken of the zinc and cobalt-doped zinc complexes confirming that the crystals were isomorphous. For example, single crystals of the zinc complex doped with 0.3% of the cobalt complex have cell parameters of $a = 11.19$ (3), $b = 14.30$ (3), and $c = 10.26$ (3) Å as measured from precession photographs.

Paramagnetic resonance measurements were made using a Varian 100-kHz X-band spectrometer with a 12-in. magnet having a 1.75-in. gap. Field measurements were made using a Harvey Wells FC-502 gaussmeter and CMC 709C frequency counter. Frequency measurements were made with a Hewlett-Packard X532A frequency meter.

All measurements were made at 4.2°K using a helium finger dewar system with the cavity at room temperature. Crystals were aligned visually on long quartz rods and could be rotated through 360° about an axis perpendicular to the field.

Results and Discussion

A. The Solid-State Molecular Structure of $[H_2B(pz)_2]_2Co$. The crystal structure consists of the packing of discrete molecules of bis[dihydrobis(1-pyrazolyl)borato]cobalt(II). The molecular configuration of one molecule of $[H_2B$ -

(19) W. C. Hamilton, *Acta Crystallogr.*, 18, 502 (1965).

(20) H. P. Hanson, F. Herman, J. D. Lea, and S. Skillman, *Acta Crystallogr.*, 17, 1040 (1964).

(21) D. H. Templeton, "International Tables for X-Ray Crystallography," Vol. III, Kynoch Press, Birmingham, England, 1962, p 215.

(22) A listing of structure factors will appear following these pages in the microfilm edition of this volume of the journal. Single copies may be obtained from the Business Operations Office, Books and Journals Division, American Chemical Society, 1155 Sixteenth Street, N.W., Washington, D. C. 20036. Remit check or money order for \$3.00 for photocopy or \$2.00 for microfiche, referring to code number INORG-73-508.

(14) F. A. Cotton, B. A. Frenz, and A. Shaver, *Inorg. Chim. Acta*, in press.

(15) B. R. McGarvey, *J. Chem. Phys.*, 53, 86 (1970).

(16) "International Tables for X-Ray Crystallography," Vol. I, Kynoch Press, Birmingham, England, 1965, p 115.

(17) L. J. Guggenberger, *Inorg. Chem.*, 7, 2260 (1968).

(18) Other computer programs used are the least-squares program SFLS5, the Busing-Levy error function program ORFFE, the Fourier program FOUR written originally by C. J. Fritchie, Jr., the Johnson plotting program ORTEP, and various local programs.

Table I. Final Positional Parameters for $[\text{H}_2\text{B}(\text{pz})_2]_2\text{Co}^a$

Atom	x	y	z
Co	0.2936 (1)	1/4	0.1102 (1)
N(1)	0.3657 (6)	0.1635 (6)	0.2389 (8)
N(2)	0.2930 (7)	0.1315 (5)	0.3404 (8)
N(3)	0.1745 (8)	0.3096 (6)	0.2273 (8)
N(4)	0.1295 (6)	0.2577 (8)	0.3236 (7)
N(5)	0.2292 (8)	0.2037 (6)	-0.0527 (9)
N(6)	0.2366 (7)	0.2662 (9)	-0.1585 (8)
N(7)	0.4264 (7)	0.3216 (6)	0.0309 (7)
N(8)	0.4063 (7)	0.3660 (6)	-0.0791 (7)
C(1)	0.3565 (10)	0.0883 (8)	0.4331 (12)
C(2)	0.4693 (12)	0.0896 (10)	0.3963 (13)
C(3)	0.4722 (9)	0.1382 (8)	0.2769 (12)
C(4)	0.0603 (8)	0.3076 (8)	0.4028 (10)
C(5)	0.0624 (10)	0.4006 (9)	0.3555 (12)
C(6)	0.1354 (8)	0.3994 (7)	0.2468 (12)
C(7)	0.1981 (9)	0.2216 (8)	-0.2697 (10)
C(8)	0.1708 (10)	0.1290 (10)	-0.2403 (14)
C(9)	0.1983 (11)	0.1227 (7)	-0.1072 (12)
C(10)	0.5071 (11)	0.3998 (8)	-0.1327 (10)
C(11)	0.5990 (11)	0.3775 (8)	-0.0481 (11)
C(12)	0.5431 (8)	0.3301 (8)	0.0492 (10)
B(1)	0.1578 (12)	0.1494 (9)	0.3216 (14)
B(2)	0.2758 (12)	0.3670 (9)	-0.1345 (13)
H(1)B(1)	0.1025	0.1112	0.3947
H(2)B(1)	0.1280	0.1162	0.2361
H(3)B(2)	0.2055	0.4036	-0.0750
H(4)B(2)	0.2803	0.4100	-0.2198
H(5)C(1)	0.3207	0.0619	0.5104
H(6)C(2)	0.5464	0.0623	0.4409
H(7)C(3)	0.5549	0.1490	0.2320
H(8)C(4)	0.0184	0.2831	0.4783
H(9)C(5)	0.0193	0.4621	0.3898
H(10)C(6)	0.1525	0.4601	0.1943
H(11)C(7)	0.1932	0.2544	-0.3501
H(12)C(8)	0.1384	0.0730	-0.2938
H(13)C(9)	0.1921	0.0557	-0.0635
H(14)C(10)	0.5160	0.4329	-0.2126
H(15)C(11)	0.6939	0.3930	-0.0562
H(16)C(12)	0.5906	0.3075	0.1225

^a The standard deviations of the least significant digits are given in parentheses.

Table II. Thermal Parameters for $[\text{H}_2\text{B}(\text{pz})_2]_2\text{Co}$ ($\times 10^4$)^a

Atom	β_{11}	β_{22}	β_{33}	β_{12}	β_{13}	β_{23}
Co	88 (1)	51 (1)	113 (1)	2 (1)	-8 (1)	7 (2)
N(1)	67 (7)	66 (6)	109 (10)	8 (6)	-4 (8)	-5 (7)
N(2)	82 (8)	45 (5)	134 (12)	-4 (6)	4 (8)	0 (6)
N(3)	121 (10)	52 (6)	121 (12)	-19 (6)	-27 (9)	20 (7)
N(4)	74 (7)	52 (5)	149 (11)	10 (8)	-16 (7)	-7 (10)
N(5)	115 (11)	45 (5)	147 (12)	-7 (6)	13 (10)	21 (7)
N(6)	84 (8)	67 (7)	124 (10)	16 (7)	-6 (7)	1 (9)
N(7)	102 (9)	76 (6)	62 (8)	25 (6)	-22 (7)	11 (6)
N(8)	88 (8)	53 (5)	113 (11)	12 (6)	-12 (8)	-16 (6)
C(1)	110 (13)	45 (7)	139 (16)	14 (8)	-20 (12)	0 (8)
C(2)	111 (16)	53 (8)	180 (21)	21 (9)	-18 (15)	3 (11)
C(3)	77 (10)	52 (7)	160 (17)	12 (7)	-7 (11)	7 (9)
C(4)	74 (10)	72 (8)	156 (15)	21 (7)	8 (11)	-7 (10)
C(5)	78 (11)	69 (10)	202 (21)	6 (8)	7 (12)	-8 (11)
C(6)	88 (11)	42 (7)	194 (17)	28 (7)	-13 (12)	-6 (9)
C(7)	81 (10)	104 (12)	116 (13)	-14 (9)	-26 (10)	-11 (10)
C(8)	107 (13)	104 (11)	191 (19)	-37 (10)	-2 (14)	-46 (13)
C(9)	137 (14)	41 (6)	212 (19)	-6 (8)	-12 (15)	-29 (11)
C(10)	109 (13)	49 (7)	106 (16)	-8 (8)	33 (11)	2 (9)
C(11)	117 (14)	65 (8)	99 (14)	-13 (9)	1 (12)	-14 (9)
C(12)	69 (10)	72 (8)	129 (15)	-5 (7)	-3 (10)	-9 (9)
B(1)	100 (15)	50 (9)	214 (25)	-21 (9)	-31 (15)	2 (12)
B(2)	107 (14)	53 (8)	170 (22)	20 (9)	-12 (14)	-17 (11)

^a The standard deviations of the least significant digits are given in parentheses. The thermal ellipsoid is of the form $\exp[-(\beta_{11}h^2 + \beta_{22}k^2 + \beta_{33}l^2 + 2\beta_{12}hk + 2\beta_{13}hl + 2\beta_{23}kl)]$. The hydrogen atom thermal parameters were fixed at 4.0 \AA^2 .

$(\text{pz})_2]_2\text{Co}$ is shown in Figure 1 which also illustrates the numbering system used here. The hydrogen atoms are

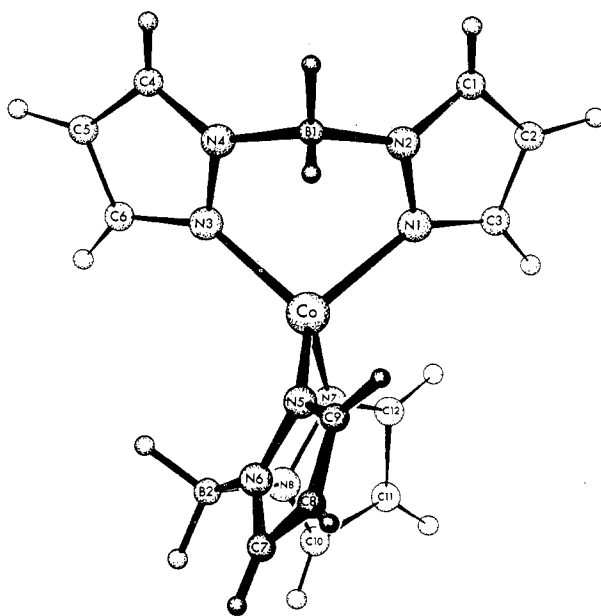


Figure 1. The molecular structure of $[\text{H}_2\text{B}(\text{pz})_2]_2\text{Co}$ viewed normal to the pseudo $S_4(\bar{4})$ axis of the local Co-N tetrahedron.

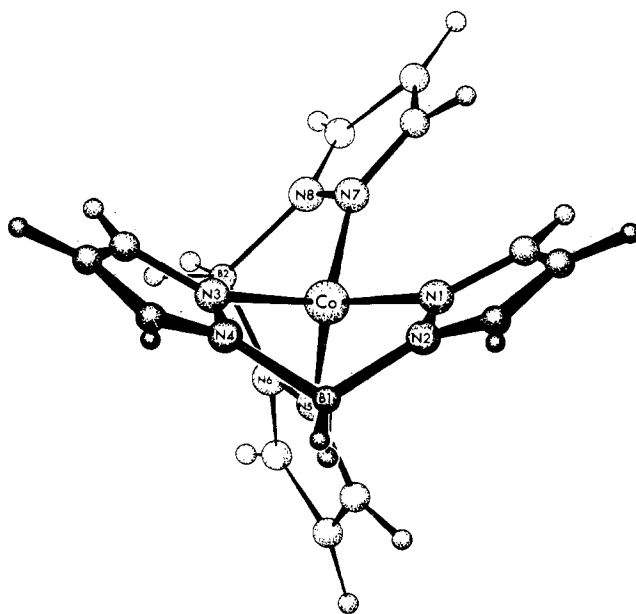


Figure 2. The $[\text{H}_2\text{B}(\text{pz})_2]_2\text{Co}$ molecule viewed in the pseudo $S_4(\bar{4})$ axis of the Co-N tetrahedron.

identified also by the atom to which they are attached (Table I). The view in Figure 1 is normal to the N(1), Co, N(3) plane, *i.e.*, in a direction normal to the pseudo $S_4(\bar{4})$ axis of the local Co-N tetrahedron. Another view of the molecular structure is shown in Figure 2 where the view is in the pseudo $S_4(\bar{4})$ direction of the tetrahedral cobalt atom.

Sets of interatomic distances and angles are given in Tables III and IV, respectively. In both tables the average is given for chemically similar quantities. The individual spread in chemically similar distances is large in some instances (attributed to the absorption effect, *vide supra*), but the average values are meaningful. The error estimates of the individual distances and angles appear to be underestimated; however, the errors of the mean values seem reasonable. The mean distances and angles are illustrated in Figure 3.

The molecular structure has two bidentate $\text{H}_2\text{B}(\text{pz})_2^-$ ligands coordinated to an essentially tetrahedral cobalt atom.

Table III. Interatomic Distances for $[\text{H}_2\text{B}(\text{pz})_2]_2\text{Co}$ (Å)^a

Co-N(1)	1.976 (8)	C(1)-C(2)	1.318 (16)
Co-N(3)	1.983 (9)	C(4)-C(5)	1.413 (13)
Co-N(5)	1.931 (10)	C(7)-C(8)	1.390 (15)
Co-N(7)	1.978 (9)	C(10)-C(11)	1.381 (15)
	Av 1.967 (12)		Av 1.376 (20)
N(1)-N(2)	1.396 (10)	C(2)-C(3)	1.403 (15)
N(3)-N(4)	1.331 (10)	C(5)-C(6)	1.379 (13)
N(5)-N(6)	1.404 (11)	C(8)-C(9)	1.397 (16)
N(7)-N(8)	1.310 (9)	C(11)-C(12)	1.356 (13)
	Av 1.360 (23)		Av 1.384 (11)
N(2)-B(1)	1.547 (14)	Co-B(1)	3.006 (14)
N(4)-B(1)	1.577 (15)	Co-B(2)	3.012 (15)
N(6)-B(2)	1.522 (18)	N(1)-N(3)	2.992 (12)
N(8)-B(2)	1.567 (14)	N(1)-N(5)	3.397 (13)
		N(1)-N(7)	3.172 (12)
	Av 1.553 (12)	N(2)-N(4)	2.573 (12)
N(1)-C(3)	1.306 (13)	N(3)-N(5)	3.293 (13)
N(3)-C(6)	1.369 (13)	N(3)-N(7)	3.466 (13)
N(5)-C(9)	1.330 (14)	N(5)-N(7)	2.905 (13)
N(7)-C(12)	1.326 (12)	N(6)-N(8)	2.509 (13)
	Av 1.333 (13)	C(3)-N(7)	3.664 (14)
N(2)-C(1)	1.335 (14)	C(3)-C(12)	3.679 (16)
N(4)-C(4)	1.328 (13)		
N(6)-C(7)	1.372 (14)		
N(8)-C(10)	1.345 (14)		
	Av 1.345 (10)		

^a Here and in Table IV the covariances were included in the estimates of the errors except where the atoms involved were in different refinement groups in which case only the variances were used. The error of the mean was calculated according to $[\sum_i n(d_i - \bar{d})^2 / n(n-1)]^{1/2}$ where d_i and \bar{d} are the function (distance or angle) and mean function, respectively.

The distortion from local tetrahedral symmetry results from the dihedral angle of 81.1° between the planes Co, N(1), N(3) and Co, N(5), N(7) (Figure 2). This distortion does not appear to arise from any special contacts but rather from the overall steric requirements of the bidentate ligands. The overall molecular symmetry is only approximately $C_2(2)$. The idealized twofold axis passes through the midpoints of N(3), N(5) and N(1), N(7). The largest deviation from $C_2(2)$ symmetry is in the tilt of the pyrazolyl rings containing N(1), N(2) and N(7), N(8); the dihedral angle between these rings is 15° instead of 0° for exact $C_2(2)$ molecular symmetry. The boron atoms are related by the idealized twofold axis with a B-Co-B angle of 145.8 (4)°.

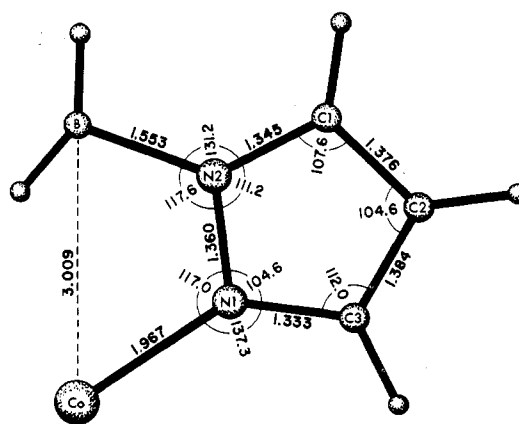
The Co-N distance of 1.967 (12) Å may be compared with the values of 1.943–1.980 (9) Å in $\text{D-}\beta_2\text{-(SSS)-[Co-(trien(S-Pro))ZnCl}_4$ (trien is triethylenetetramine and Pro is a proline residue) and 2.129 (7) Å in the $[\text{HB}(\text{pz})_3]_2\text{Co}^{12}$ structure. The difference between the Co-N distances in the bidentate and tridentate pyrazolylborato complexes probably arises from the change in coordination number and the increased steric requirements of the tridentate ligand.

A detailed comparison of the observed stereochemistry of transition metal pyrazolylborates is given in Table V. Another structure, $\text{B}(\text{pz})_4\text{Mo}(\text{CO})_2\text{C}_5\text{H}_5$, determined independently by two groups^{24,25} was not included in Table V because one determination is not yet published²⁴ and the other is based on a preliminary refinement²⁵ and hence lacks the precision of the remaining structures. The pyrazolylborate framework is fairly constant in these structures; in fact, it is fairly constant even when the simple

(23) H. C. Freeman, L. G. Marzilli, and I. E. Maxwell, *Inorg. Chem.*, **9**, 2408 (1970).

(24) E. M. Holt, S. L. Holt, and M. Nemiroff, private communication.

(25) J. L. Calderon, F. A. Cotton, and A. Shaver, *J. Organometal. Chem.*, **127** (1972).

Figure 3. Mean ligand distances and angles for $[\text{H}_2\text{B}(\text{pz})_2]_2\text{Co}$.

metal pyrazoles are included. The average ligand geometry including the structures in Table V and the metal pyrazole structures of $\text{Ni}(\text{Hpz})_4\text{Cl}_2$,²⁶ $\text{Ni}(\text{Hpz})_2\text{Br}_2$,²⁷ and $\text{Ni}(\text{Hpz})_6\text{-(NO}_3)_2$ ²⁸ has 1.358 (3) Å for N(1)-N(2), 1.347 (1) Å for N(2)-C(1), 1.336 (3) Å for N(1)-C(3), 1.372 (5) Å for C(1)-C(2), 1.391 (3) Å for C(2)-C(3), 110.5 (3)° for N(1)-N(2)-C(1), 105.9 (4)° for N(2)-N(1)-C(3), 107.7 (3)° for N(2)-C(1)-C(2), 110.4 (3)° for N(1)-C(3)-C(2), and 105.3 (3)° for C(1)-C(2)-C(3). The interatomic distances in uncoordinated pyrazole²⁹ are 1.35 Å for N(1)-N(2), 1.33 Å for N(2)-C(1), 1.34 Å for N(1)-C(3), 1.36 Å for C(1)-C(2), and 1.38 Å for C(2)-C(3). Differences in pyrazole, metal-pyrazole, and metal-pyrazolylborate ligand geometries are minor and of borderline statistical significance. Comparison of the bidentate and tridentate cobalt and molybdenum complexes (Table V) suggests that the metal-nitrogen distance is dependent more on the overall metal coordination number than the chelating characteristics of the ligand. The short Mo-B distance in $\text{H}_2\text{B}[3,5\text{-(CH}_3)_2\text{pz}]_2\text{Mo}(\text{CO})_2\text{-}\pi\text{-C}_3\text{H}_5$ was commented on by the authors,¹⁰ who suggested the possibility of a Mo-H interaction. A three-center, two-electron B-H-Mo type bond was established for $\text{H}_2\text{B-}[(\text{CH}_3)_2\text{pz}]_2\text{Mo}(\text{CO})_2(\text{C}_7\text{H}_7)$.¹¹

The best least-squares planes through the pyrazolyl rings are given in Table VI; these rings are planar within experimental error. The boron atoms are nearly in the ring planes, but they were not included in the plane calculation as there is some tendency for slight rotation of the plane about the N-N direction as observed in the $[\text{HB}(\text{pz})_3]_2\text{Co}^{12}$ structure. The nearly planar pyrazolyl rings with N(1), N(2) and N(7), N(8) (dihedral angle is 15.0°) give the shortest contacts between coordinated ligands [H(7)C(3)-H(16)C(12) is 2.6 Å], but these contacts do not appear to influence the cobalt stereochemistry.

A stereoview of the crystal structure is shown in Figure 4, illustrating also the thermal ellipsoids which are plotted at the 50% probability level. The root-mean-square amplitudes of vibration varied from 0.16 to 0.38 Å; the most anisotropic atom is C(6) with minimum and maximum root-mean-square amplitude components of 0.16 and 0.32 Å, respectively.

The molecules are separated by the normal van der Waals

(26) C. W. Reimann, A. D. Mighell, and F. A. Mauer, *Acta Crystallogr.*, **23**, 135 (1967).

(27) A. D. Mighell, C. W. Reimann, and A. Santoro, *Acta Crystallogr., Sect. B*, **25**, 595 (1969).

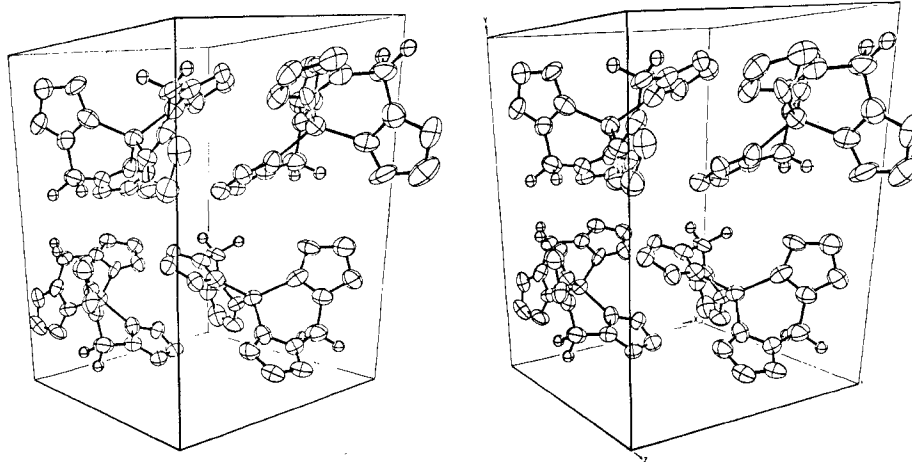
(28) C. W. Reimann, A. Santoro, and A. D. Mighell, *Acta Crystallogr., Sect. B*, **26**, 521 (1970).

(29) J. Berthow, J. Elguero, and C. Rerat, *Acta Crystallogr., Sect. B*, **26**, 1880 (1970).

Table IV. Selected Interatomic Angles for $[\text{H}_2\text{B}(\text{pz})_2]_2\text{Co}$ (deg)^a

N(1)-Co-N(3)	98.2 (3)	N(1)-N(2)-B(1)	115.1 (9)
N(1)-Co-N(5)	120.8 (4)	N(3)-N(4)-B(1)	117.4 (9)
N(1)-Co-N(7)	106.7 (3)	N(5)-N(6)-B(2)	119.5 (9)
N(3)-Co-N(5)	114.5 (4)	N(7)-N(8)-B(2)	118.3 (9)
N(3)-Co-N(7)	122.1 (4)	N(2)-B(1)-N(4)	Av 117.6 (9)
N(5)-Co-N(7)	96.0 (4)	N(6)-B(2)-N(8)	110.9 (9)
B(1)-Co-B(2)	145.8 (4)		108.6 (9)
Co-N(1)-N(2)	117.4 (6)		Av 109.8 (12)
Co-N(3)-N(4)	117.5 (7)	N(1)-C(3)-C(2)	112.0 (10)
Co-N(5)-N(6)	115.1 (6)	N(3)-C(6)-C(5)	108.6 (8)
Co-N(7)-N(8)	118.1 (6)	N(5)-C(9)-C(8)	114.2 (11)
	Av 117.0 (7)	N(7)-C(12)-C(11)	113.4 (9)
			Av 112.0 (12)
Co-N(1)-C(3)	138.2 (6)	N(2)-C(1)-C(2)	107.6 (11)
Co-N(3)-C(6)	134.8 (6)	N(4)-C(4)-C(5)	106.6 (9)
Co-N(5)-C(9)	139.1 (6)	N(6)-C(7)-C(8)	109.4 (11)
Co-N(7)-C(12)	137.0 (5)	N(8)-C(10)-C(11)	106.8 (10)
	Av 137.3 (9)		Av 107.6 (6)
N(1)-N(2)-C(1)	111.6 (8)	C(1)-N(2)-B(1)	133.3 (9)
N(3)-N(4)-C(4)	111.9 (9)	C(4)-N(4)-B(1)	130.6 (10)
N(5)-N(6)-C(7)	108.9 (9)	C(7)-N(6)-B(2)	131.5 (11)
N(7)-N(8)-C(10)	112.3 (8)	C(10)-N(8)-B(2)	129.3 (9)
	Av 111.2 (8)		Av 131.2 (8)
N(2)-N(1)-C(3)	102.8 (8)	C(1)-C(2)-C(3)	106.1 (12)
N(4)-N(3)-C(6)	107.0 (9)	C(4)-C(5)-C(6)	105.9 (10)
N(6)-N(5)-C(9)	104.2 (9)	C(7)-C(8)-C(9)	102.9 (11)
N(8)-N(7)-C(12)	104.3 (8)	C(10)-C(11)-C(12)	103.3 (11)
	Av 104.6 (9)		Av 104.6 (8)

^a Footnote to Table III applies. When the three atoms were not in the same refinement group Cruickshank's formula ("International Tables for X-Ray Crystallography," Vol. II, Kynoch Press, Birmingham, England, 1959, p 331) was used to estimate the error.

Figure 4. Stereoview of the $[\text{H}_2\text{B}(\text{pz})_2]_2\text{Co}$ crystal structure.

contacts. The shortest intermolecular contacts were 3.434 Å for nonhydrogen atom contacts, 2.71 Å for hydrogen to nonhydrogen atom contacts, and 2.35 Å for hydrogen atom contacts (between H(2)B(1) and H(10)C(6) on a neighboring molecule).

B. Paramagnetic Resonance Data. The apparent g values (g_x' , g_y' , g_z') and hyperfine coupling constants measured from the powder spectra are given in Table VII. The complexes appear to fall into two categories, those with $A_z \approx 0$, $g_z' \approx 6.9$, and $(g_x' + g_y')/2 \approx 1$ and those with $A_z \approx 0.015 \text{ cm}^{-1}$, $g_z' \approx 7.4$, and $(g_x' + g_y')/2 \approx 2.15$. Examples of these two types of powder spectra are shown in Figures 5 and 6.

Single-crystal data were obtained for the parent complex with the corresponding zinc complex as the host lattice. The data will not be examined in detail at this time since, as will appear from the discussion, it is not possible to define all the parameters of the spin Hamiltonian unambiguously from experiments at 4.2°K. For spectra taken by rotating the crystal about the a or b axes, with the axis of

rotation perpendicular to the magnetic field, a sharp single line is observed at $g_{\text{eff}} = 6.59$ when the c axis is along the field. A rotation about a which inclines c in a direction making an angle of close to 5° with the field splits the resonance into two sharp lines, the one at lower field having g_{eff} close to the value of g_z' for the powder spectra. A similar effect is found for a rotation about b which inclines c at 14° to the field. It is clear from these results that the direction of g_z is close to the direction of the c axis. In all these cases, the hyperfine splitting is small and unresolved.

The direction of g_x' is close to the direction of the b axis with the hyperfine splitting parameter $A_x \approx 0.002 \text{ cm}^{-1}$ and similarly the direction of g_y' is close to the a axis with $A_y \approx 0.002 \text{ cm}^{-1}$. An upper limit on A_z (for which no hyperfine structure is resolved) is also $\sim 0.002 \text{ cm}^{-1}$.

It is of interest in light of the epr work to describe the orientation of the molecule with respect to the cell edges. We have done this by attaching an orthogonal coordinate system to the molecule in the following manner. We start with vectors A in the S_4 direction (N(5)-N(7) and N(2)-N(4))

Table V. Comparison of Structural Data for Metal Pyrazolylborates^a

Atoms	[H ₂ B(pz) ₂] ₂ Co ^b	[HB(pz) ₃] ₂ Co ^c	H ₂ B[(CH ₃) ₂ pz] ₂ - Mo(CO) ₂ (C ₃ H ₅) ₂ ^d	HB(pz) ₃ Mo(CO) ₂ - N ₂ C ₆ H ₈ ^e	H ₂ B[(CH ₃) ₂ - pz] ₂ Mo(CO) ₂ - (C ₇ H ₇) ^f	HB(pz) ₃ (COCH ₃) ₂ - Fe(CO) ₂ ^g	Mean
Distance, Å							
M-N(1)	1.967 (12)	2.129 (7)	2.214 (37)	2.218 (7)	2.201	2.024	
N(1)-N(2)	1.360 (23)	1.364 (3)	1.364 (12)	1.361 (12)	1.376 (4)	1.359 (1)	1.364 (3)
N(2)-C(1)	1.345 (10)	1.339 (15)	1.353 (11)	1.348 (1)	1.345 (6)	1.350 (3)	1.347 (2)
N(1)-C(3)	1.333 (13)	1.330 (15)	1.354 (5)	1.336 (6)	1.348 (4)	1.340 (5)	1.340 (4)
C(1)-C(2)	1.376 (20)	1.379 (25)	1.393 (5)	1.380 (3)	1.389 (5)	1.364 (5)	1.380 (4)
C(2)-C(3)	1.384 (11)	1.393 (23)	1.385 (2)	1.403 (5)	1.410 (5)	1.383 (8)	1.393 (5)
M-B	3.009 (3)	3.195 (4)	2.81	3.345		3.147 (5)	
Angle, Deg							
N(1)-M-N(3)	97.1 (11)	85.5 (2)	80.87 (16)	81.8 (2)	80.4 (1)	86.8 (17)	
M-N(1)-N(2)	117.0 (7)	119.1 (3)	109.3 (8)	120.7 (3)	108.6 (8)	120.0 (8)	
M-N(1)-C(3)	137.3 (9)	134.7 (11)	143.5 (13)	131.9 (1)		133.6 (6)	
N(1)-N(2)-C(1)	111.2 (8)	109.9 (11)	110.4 (4)	109.5 (1)	109.6 (3)	109.3 (1)	110.0 (3)
N(2)-N(1)-C(3)	104.6 (9)	106.0 (9)	106.9 (3)	107.3 (3)	107.3 (2)	106.3 (3)	106.4 (4)
N(2)-C(1)-C(2)	107.6 (6)	109.0 (13)	106.8 (3)	108.4 (1)	108.6 (3)	108.7 (2)	108.2 (3)
N(1)-C(3)-C(2)	112.0 (12)	111.2 (10)	109.1 (3)	109.3 (2)	109.2 (4)	110.5 (3)	110.2 (5)
C(1)-C(2)-C(3)	104.6 (8)	104.1 (8)	106.8 (1)	105.1 (1)	105.4 (3)	105.2 (3)	105.2 (4)

^a Averages were taken for chemically similar distances and angles; the errors were estimated as in Table III. ^b Bidentate ligand; this work. ^c Tridentate ligand; see ref 12. ^d Bidentate ligand; see ref 10. ^e Tridentate ligand, see ref 13. ^f Bidentate ligand; see ref 11. ^g Tridentate ligand; see ref 14.

midpoints) and *B* in the *C*₂ direction (N(3)-N(5) and N(1)-N(7) midpoints). We then form orthogonal molecular axes *X*_m, *Y*_m, *Z*_m, *i.e.*

$$X_m = A$$

$$Y_m = (A \times B) \times A$$

$$Z_m = A \times B$$

The result is that *X*_m is in the *S*₄ direction and *Y*_m is in the *C*₂ direction normal to *S*₄. The orientation of the molecular axes with respect to the cell edges is given by the following 3 × 3 matrix labeled by rows and columns.

	<i>X</i> _m (<i>S</i> ₄)	<i>Y</i> _m (<i>C</i> ₂)	<i>Z</i> _m
<i>a</i>	109.8°	19.8°	88.4°
<i>b</i>	104.6°	96.8°	16.1°
<i>c</i>	24.9°	71.5°	74.0°

Since the *S*₄ and *C*₂ axes are not rigorously required by the symmetry of the crystal lattice, it is not necessary for the principal axes of the *g*' tensor and *A* tensor to lie along them. It does, however, seem clear from the discussion earlier in this section together with the angles in the matrix that there must be a quite close correspondence between the directions *X*_m, *Y*_m, and *Z*_m and the directions of *g*_{*z*'}, *g*_{*y*'}, and *g*_{*x*'}, respectively.

The single-crystal data do serve to show that the three principal absorptions in the powder spectra correspond to transitions between the same pair of levels.

The electronic ground state of the Co²⁺ ion in a regular tetrahedral ligand field is ⁴A₂. Under the combined influence of spin-orbit coupling and low-symmetry components in the ligand field, the ground state is split into two Kramers doublets. If the ligand field distortion is axial, the paramagnetic resonance properties of the ground-state manifold can then be described by a spin Hamiltonian of the form

$$\mathcal{H} = \beta g_{\parallel} S_z H_z + \beta g_{\perp} (S_x H_x + S_y H_y) + D [S_z^2 - 1/3 S(S+1)]$$

2*D* is the separation between the Kramers doublets (the zero-field splitting) and is usually of the order of a few cm⁻¹. The doublets can be characterized by the *S*_{*z*} quantum numbers *S*_{*z*} = ±3/2 and *S*_{*z*} = ±1/2. The most thoroughly studied system involving a tetrahedral cobalt complex is Cs₃CoCl₅³⁰ where transitions between the ±3/2 doublet and the ±1/2

Table VI

Least-Squares Planes for [H ₂ B(C ₃ N ₂ H ₃) ₂] ₂ Co ^a	
Plane 1: Co, N(1), N(3)	Equation: 0.669 <i>X</i> + 0.701 <i>Y</i> + 0.247 <i>Z</i> - 4.978 = 0
Plane 2: Co, N(5), N(7)	Equation: -0.589 <i>X</i> + 0.806 <i>Y</i> - 0.065 <i>Z</i> - 0.866 = 0
Plane 3: N(1), N(2), C(1), C(2), C(3)	Equation: 0.119 <i>X</i> + 0.868 <i>Y</i> + 0.482 <i>Z</i> - 3.694 = 0
Plane 4: N(3), N(4), C(4), C(5), C(6)	Equation: 0.795 <i>X</i> + 0.196 <i>Y</i> + 0.574 <i>Z</i> - 3.762 = 0
Plane 5: N(5), N(6), C(7), C(8), C(9)	Equation: 0.948 <i>X</i> - 0.253 <i>Y</i> - 0.192 <i>Z</i> - 1.838 = 0
Plane 6: N(7), N(8), C(10), C(11), C(12)	Equation: -0.141 <i>X</i> + 0.857 <i>Y</i> + 0.495 <i>Z</i> - 3.422 = 0

Atom Deviations from Planes, Å							
	Plane 3	Plane 4	Plane 5	Plane 6			
N(1)	-0.006	N(3)	-0.010	N(5)	-0.037	N(7)	-0.008
N(2)	0.000	N(4)	0.009	N(6)	0.024	N(8)	0.010
C(1)	0.006	C(4)	-0.004	C(7)	-0.005	C(10)	-0.008
C(2)	-0.009	C(5)	-0.002	C(8)	-0.018	C(11)	0.002
C(3)	0.009	C(6)	0.007	C(9)	0.035	C(12)	0.004
Co	0.337	Co	0.198	Co	0.160	Co	-0.272
B(1)	-0.051	B(1)	-0.054	B(2)	0.029	B(2)	-0.051
Dihedral Angles between Planes, Deg							
1-2	81.1	3-6	15.0	5-6	116.5		
3-4	57.2	4-5	53.6				
3-5	101.5	4-6	70.1				

^a The equations are expressed in cartesian coordinates relative to *a*, *b*, and *c*. The atoms defining the planes are listed with the plane equations.

Table VII. Hyperfine Splittings and Effective *g* Values

Compd	<i>A</i> _{<i>z</i>} , cm ⁻¹	<i>g</i> _{<i>z</i>'}	<i>g</i> _{<i>y</i>'}	<i>g</i> _{<i>x</i>'}
Co[H ₂ B(pz) ₂] ₂	~0	6.90	1.13	0.95
Co[H ₂ B[3,4,5-(CH ₃) ₃ (pz) ₂] ₂	~0	6.95	1.02	0.85
Co[(C ₆ H ₅) ₂ B(pz) ₂] ₂	0.016	7.47	2.28	2.03
Co[H ₂ B[3,5-(CH ₃) ₂ (pz) ₂] ₂	0.013	7.35	2.30	2.00

doublet have been observed directly giving an accurate measure of the zero-field splitting. In this study magnetic fields up to 90 kG and microwave frequencies up to 120 kHz were employed. Additionally, a complete theoretical treatment has been carried out including all the states of the

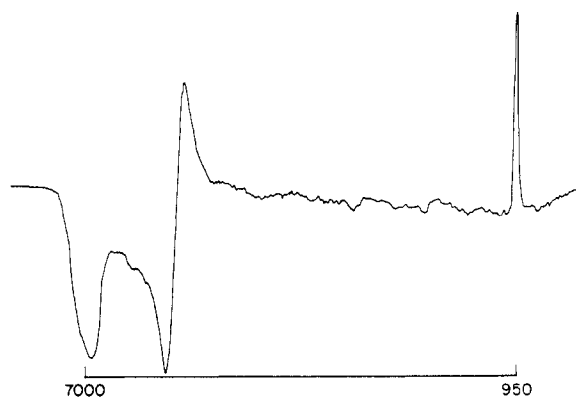


Figure 5. Epr spectrum (9.3 kHz) of a magnetically dilute powder sample of $[\text{H}_2\text{B}(\text{pz})_2]_2\text{Co}$ at 4.2°K . Horizontal scale in gauss.

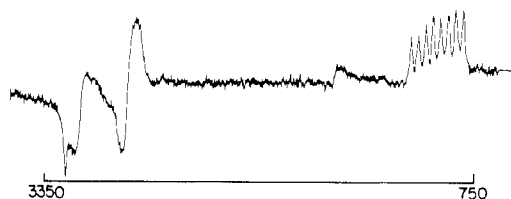


Figure 6. Epr spectrum (9.3 kHz) of a magnetically dilute powder sample of $\text{Co}\{\text{H}_2\text{B}[3,5-(\text{CH}_3)_2(\text{pz})_2]_2\}_2$ at 4.2°K . Horizontal scale in gauss.

d^7 configuration, fitting both the epr data and polarized single-crystal optical data obtained at liquid helium temperature.³¹ For Cs_3CoCl_5 the parameters in the spin Hamiltonian are

$$g_{\parallel}(\pm 1/2) = 2.38 \pm 0.01$$

$$g_{\perp}(\pm 1/2) = 2.30 \pm 0.01$$

$$2D = -8.6 \pm 0.10 \text{ cm}^{-1}$$

The system is required by the space group to have axial symmetry and the sign of the zero-field splitting leaves the $\pm 3/2$ level lowest. It is instructive to examine the behavior of the energy levels in the axial system as a function of D . With fields along the parallel direction the splittings of the $\pm 1/2$ and $\pm 3/2$ levels are independent of D , with values $g_{\parallel}\beta H$ and $3g_{\parallel}\beta H$, respectively. The value of g_{\parallel} is expected to be in the range 2.2–2.4, depending on the position of the $^4\text{B}_2$ component of the first excited state $^4\text{T}_2$. The simple perturbation formula is

$$g_{\parallel} = 2 + 8\zeta/[3E(^4\text{B}_2)]$$

where ζ is the one-electron spin-orbit coupling parameter. We therefore expect a strong resonance for the spin-allowed $1/2 \leftrightarrow -1/2$ transition in the region $g' = 2.3$ for most tetrahedral Co^{2+} complexes when the field is along the parallel axis. It is clear from the single-crystal and powder studies reported for the pyrazolylborates that no such resonance occurs. There appear to be only two possible explanations for this observation: (a) the Orbach process is still so efficient at 4.2°K that T_{1e} is short enough for the resonance to be broadened beyond detection; (b) the $\pm 1/2$ level is not appreciably thermally populated at 4.2°K . If explanation (b) were correct, then clearly the observed transitions with the effective g values given in Table VII have to correspond to the $\pm 3/2$ doublet. This transition is forbidden in first order but has been detected in the accurately axial case²⁸ and can have a larger transition probability for rhombic

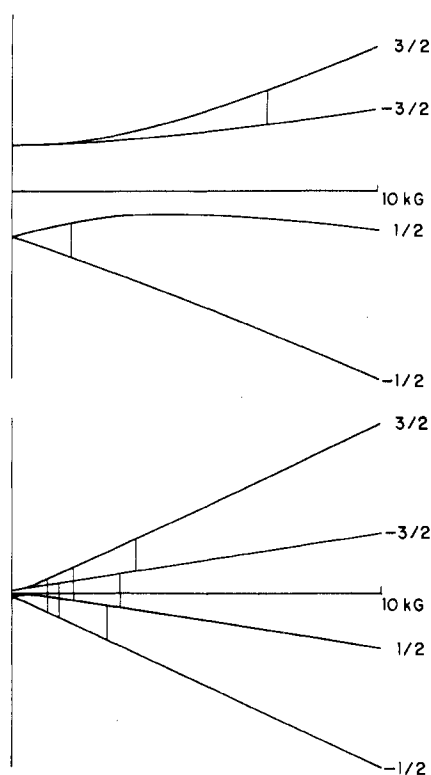


Figure 7. Calcomp outputs for the energy levels of the quartet ground-state manifolds of $[\text{H}_2\text{B}(\text{pz})_2]_2\text{Co}$ and $\{\text{H}_2\text{B}[3,5-(\text{CH}_3)_2(\text{pz})_2]_2\}_2\text{Co}$, respectively, as a function of field using the spin Hamiltonian parameters which give the experimentally observed apparent g values. The H_0 field is in the x direction and possible transitions (9.3 kHz) are shown as vertical lines. The epr parameters used in the upper part of the figure are $D = 0.43 \text{ cm}^{-1}$, $E = 0$, $g_x = 2.1$, $g_y = 2.5$, and $g_z = 2.3$. For the lower part, $D = 0.043 \text{ cm}^{-1}$, $E = 0$, $g_x = 2.62$, $g_y = 2.27$, and $g_z = 2.45$.

symmetry. $g_z' = 6.90$, the observed effective g value with the field close to the pseudo S_4 axis of the molecule, would then correspond to $3g_{\parallel}$ giving the reasonable result

$$g_{\parallel} = 2.30$$

For large D , $g_{\perp}(\pm 3/2) \approx 0$ so that the observation of $(g_x + g_y)/2 \approx 1.0$ indicates that D is too small for explanation (b) to be correct.

A best fit to the $\pm 3/2$ transition with $g_{\parallel} = 2.30$, assuming axial symmetry and varying g_{\perp} in the range 2.2–2.4, gives $D \approx 0.4 \text{ cm}^{-1}$

It may be noted that $g_{\perp}'(\pm 3/2)$ is quite sensitive to the value of D .

Following this approximate treatment, a complete fit using the general rhombic Hamiltonian

$$\mathcal{H} = \beta\mathbf{S} \cdot \mathbf{g} \cdot \mathbf{H} + D[S_z^2 - 1/3S(S+1)] + 1/2E(S_+^2 + S_-^2)$$

was attempted. A general program has been written to evaluate the energy levels corresponding to this Hamiltonian as a function of H for any S . The program searches for transitions which meet the resonance condition $\nu = 9.3 \text{ kHz}$ and produces Calcomp plots of the energy levels as a function of field with vertical lines indicating the fields at which the resonance condition is met. Since the g tensor is to a first approximation axial, the behavior of the levels with the field in the z direction is straightforward. In the x and y directions strong mixing of the zero-field levels takes place allowing, as indicated above, a reasonably accurate de-

(31) J. P. Jesson, *J. Chem. Phys.*, **48**, 161 (1968).

termination of D . The data in the present case are not sufficient to define g_x , g_y , and E separately. Equally good fits can be obtained with the following parameter sets for $\text{Co}[\text{H}_2\text{B}(\text{pz})_2]_2$, in the one case holding $E = 0$ and in the other holding g_x and g_y equal to g_z .

$$\begin{array}{ll} D = 0.43 \text{ cm}^{-1} & D = 0.44 \text{ cm}^{-1} \\ E = 0 & E = -0.19 \text{ cm}^{-1} \\ g_x = 2.10 & g_x = 2.30 \\ g_y = 2.50 & g_y = 2.30 \\ g_z = 2.30 & g_z = 2.30 \end{array}$$

The calculated values of g_x' , g_y' , and g_z' are 0.95, 1.13, and 6.90, respectively. Similar ambiguity is, of course, found for $\{\text{H}_2\text{B}[3,5\text{-(CH}_3)_2(\text{pz})_2]_2\}_2\text{Co}$.

Figure 7 shows the Calcomp outputs for the two molecules when the H_0 field is in the x direction. For the first compound there is only one possible high-field transition; for the second compound the calculated zero-field splitting is an order of magnitude smaller and there are six potentially observable transitions. Under these latter conditions it is difficult to see why only one transition is observed. The levels are heavily mixed, they are all thermally populated at 4.2°K, and one might anticipate similar relaxation times and transition probabilities for the possible transitions.

The interpretation given above appears to be the most likely on the basis of the data currently available but cannot be regarded as unambiguous. Experiments which might help to resolve this problem are (a) epr studies below 4.2°K where T_{1e} for the $\pm 1/2$ doublet may be shortened enough to allow detection of the $\pm 1/2$ resonance, (b) studies of the temperature dependence and anisotropy of the magnetic susceptibility near 4.2°K, and (c) epr studies at K-band frequencies. We are not currently equipped to perform these experiments

but hope eventually to do some or all of them.

Conclusions

Single-crystal X-ray data, including the molecular and crystal structures, have been presented for $[\text{H}_2\text{B}(\text{pz})_2]_2\text{Co}$. The Co coordination is essentially tetrahedral, but the distortions from a regular tetrahedron are significant (96–122° N-Co-N angles). The overall molecular symmetry is idealized $C_2(2)$. There are no unusual intermolecular contacts. Individual structural parameters are compared with related compounds.

The epr studies illustrate some of the difficulties which may be encountered in using this approach to define the magnetic properties of the central metal ion and seem to represent a unique case in tetrahedral Co^{2+} where a forbidden transition is observed but the principal allowed transition is not.

The quite large variation in the apparent g values and in the zero-field splittings in the substituted complexes also suggest that caution must be exercised in transferring magnetic data obtained in the solid state to the analysis of solution properties such as isotropic resonance shifts. It is possible that these changes in g values are direct effects of the substituents at the molecular level, but it is also possible that they are due to crystal packing effects. A clearer definition of the magnetic properties of the central metal ion in these complexes will be required before detailed interpretation of the isotropic nuclear resonance shifts of the ligand protons can be undertaken.

Registry No. $[\text{H}_2\text{B}(\text{pz})_2]_2\text{Co}$, 37668-73-8.

Acknowledgment. We wish to thank Professor F. A. Cotton for communicating his results prior to publication.

Contribution from Ames Laboratory—USAEC and the Department of Chemistry, Iowa State University, Ames, Iowa 50010

Crystal Structure of Hexaamminecobalt Nonafluoroantimonate(III)

DONALD R. SCHROEDER and ROBERT A. JACOBSON*

Received August 15, 1972

The crystal structure of hexaamminecobalt nonafluoroantimonate(III), $\text{Co}(\text{NH}_3)_6\text{Sb}_2\text{F}_9$, has been solved by single-crystal X-ray diffraction techniques at room temperature ($25 \pm 2^\circ$) using three-dimensional scintillation counter data and a full-matrix anisotropic least-squares refinement procedure ($R = 0.060$). The compound crystallizes in the monoclinic crystal system of space group $P2_1/c$, with cell lattice parameters $a = 7.223$ (5), $b = 7.298$ (3), $c = 12.432$ (7) Å and $\beta = 93.15$ (8)°. The asymmetric unit consists of one octahedral $\text{Co}(\text{NH}_3)_6^{3+}$ ion and one distorted $\text{Sb}_2\text{F}_9^{3-}$ ion. The $\text{Sb}_2\text{F}_9^{3-}$ ion resembles two octahedra sharing a corner with each octahedron possessing a lone pair. It was also found that the bridging fluorine in this compound is statistically disordered. The bridge is asymmetric with Sb-F bonds of 2.249 (12) and 2.449 (4) Å. The Sb-F bond length opposite the lone pair is 1.948 (7) Å while the Sb-F distance opposite the bridging fluorine is 2.015 (5) Å. The remaining two Sb-F bonds are trans to one another with distances of 2.080 (11) and 2.078 (8) Å, respectively. The mean Co-N distance is 1.990 (5) Å.

Introduction

The crystal structure investigation of hexaamminecobalt nonafluoroantimonate(III) was undertaken as part of a series of investigations of halo-coordinated antimony compounds being performed in this laboratory.¹⁻⁶ The stereo-

chemistry and the role, if any, the lone pair plays in the coordination sphere are of particular interest in these studies.

(3) S. L. Lawton and R. A. Jacobson, *Inorg. Chem.*, **5**, 743 (1966).

(4) C. R. Hubbard and R. A. Jacobson, *Inorg. Chem.*, **11**, 2247 (1972).

(5) S. K. Porter and R. A. Jacobson, *J. Chem. Soc. A*, 1356 (1970).

(6) W. Pflaum and R. A. Jacobson, to be submitted for publication.

(1) C. R. Hubbard and R. A. Jacobson, *Proc. Iowa Acad. Sci.*, **75**, 85 (1968).

(2) S. L. Lawton and R. A. Jacobson, *Inorg. Chem.*, **7**, 2124 (1968).